Chapter 25
Investigation of 3D Printed Jet Fuel Atomizer

Raja Marudhappan, U. Chandrasekhar and K. Hemachandra Reddy

Abstract The simplex atomizer of an annular combustion chamber of an 1100-kW class aero-derivative turboshaft engine is designed. Three-dimensional CAD model of the atomizer is made. An attempt is made to fabricate the atomizer model in 3D printing using acrylonitrile butadiene styrene and fused deposition modeling technique. The quality of the 3D printed atomizer is studied for the suitability of functional testing. It is found that the surface finish and the smallest structural features of the 3D printed model are not meeting the functional requirements. Hence, the atomizer manufactured by conventional machining is considered in numerical modeling and performance testing using Jet A fuel. The transient 2D axisymmetric flow analysis is performed by solving Navier–Stokes equations. The fuel–air interface is tracked by following the Euler–Euler approach and using the volume of fluid (VOF) surface tracking mathematical model. The velocity fields across the swirl chamber and in the near exit zone are presented. The air core formation and hollow cone spray obtained from numerical modeling are compared to previously published reports. The atomizer is tested in an atmospheric test facility to assess the quality of jet penetration and hollow cone spray formation. The observed performance characteristics are compared to the published literature and found in order. Alternative techniques for 3D printing of the atomizer and the related issues are discussed.

Keywords 3D printing · Atomizer · Annular combustor · Turboshaft · Numerical modeling

R. Marudhappan (✉) · K. Hemachandra Reddy
JNTUA, Anantapur 515002, India
e-mail: raja.marudhappan@gmail.com

U. Chandrasekhar
Vel Tech University, Chennai 600062, India

Nomenclature

x, y, z	Spatial coordinates
u, v, w	Instantaneous velocity along spatial coordinates x, y, z
V	Velocity vector field
ρ	Density
p	Pressure
τ	Shear stress
β	Liquid volume fraction
$\dot{m}_{ab}$	Mass transfer from phase a to phase b
$\dot{m}_{ba}$	Mass transfer from phase b to phase a
q	Body force per unit mass

25.1 Introduction

Atomization converts the bulk of fuel into small droplets. The atomization process comprises two separate processes. The first process also called the primary atomization converts the fuel stream into shreds and ligaments. Further secondary atomization leads to breaking of larger drops and globules resulted from primary atomization. There are two mechanisms of atomization of liquids, viz. classical mechanism and prompt mechanism. When the velocity of flow is lesser, classical atomization predominates. Prompt mechanism occurs when the flow velocity is larger. The atomization mechanism in gas turbine engines generally follows prompt mechanism. The major task of the atomizer is to provide sufficiently larger surface area by forming an increased number of fuel droplets. Hence, drop sizes and drop size distribution are important performance requirements of the atomizer. Another task of the atomizer is to distribute the drops as per the requirement in the combustion chamber in order to achieve a well-controlled air–fuel mixture distribution and rapid mixing.

25.2 Literature Review

Atomization can be achieved through different methods. These methods involve many basic processes such as hydraulics of flow inside the atomizers. The hydraulics govern the turbulence of the emerging liquid spray. The shape, penetration, and number density of drops are controlled by the development of the jet and the growth of small disturbances leading to the disintegration of the sheet into ligaments and then drops [1].

Atomizers are broadly classified into three distinct categories based on the basic process involved. The pressure atomization is achieved by forcing the liquid through a narrow orifice to obtain high velocity. The thin fluid atomization uses high-velocity air stream to disintegrate fuel jet. Rotary atomizers employ centrifugal forces to produce liquid sheet while flowing along the surface of a rotating disk [2].

The pressure atomization is the simplest method to atomize the liquid fuel. The pressure energy of the liquid is converted into kinetic energy inside the nozzle, and the liquid is forced through the orifice. When the liquid enters the orifice with a tangential velocity component, a hollow cone spray emerges in the downstream of the orifice. The spray cone angle of 60–100° can be achieved by controlling the flow properties closely.

The internal flow of water in a scaled pressure swirl atomizer is modeled numerically and experimentally by Hansen et al. [3]. The study is conducted to validate the applicability of commercial CFD code CFX-4.3 in modeling the atomization process. Laser Doppler anemometry (LDA) is used in experiments for measuring the flow velocity. The study reported the presence of Rankine-vortex-like phenomena in tangential velocity profile. The study is made based on turbulence and laminar flow. The numerical simulations managed to capture the characteristics of pressure swirl atomizer by capturing the air core and thin film of fluid in the orifice exit region.

Rezaeimoghaddam et al. [4] studied the effects of shear thinning and shear thickening fluids in a pressure swirl atomizer. The fluid flow inside the atomizer is simulated by solving Navier–Stokes equations time-independently and solving the transport equation for volume fraction by VOF model. The numerical study used different sizes of orifices. The results obtained from the numerical study are compared to Ma's experimental data [5]. The comparison shows that the tangential velocity decreases when the power law index increases.

The atomization of Jet A-1 fuel in a commercial pressure swirl atomizer is experimentally investigated by Marchione et al. [6]. Phase Doppler anemometry (PDA) is used for the characterization of drop sizes and velocity. The fluctuation of spray behavior is examined with a high-speed charge-coupled camera. The analysis of the digital image has confirmed that the instantaneous spray cone angle is approximately equal to the one obtained with a PDA. Two oscillation modes at 100 and 1800 Hz are reported.

Numerical simulation of the internal flow of swirl atomizer under ambient pressure is reported by Fu [7]. VOF method is used to track the interface of liquid and air. The steady-state flow analysis is performed on a 2D axisymmetric model. The effect of inlet pressure fluctuations on a spray cone angle and flow rate is reported. The VOF model is able to capture the liquid–air interface.

Mkvik et al. [8] performed a numerical investigation on a twin-fluid atomizer internal flow. The viscous aqueous Maltodextrin solution is used in the experiments. Twin-fluid atomizers use a pressurized gas stream to enhance the jet breakup. The simulation is performed on a commercial CFD code. The investigation reported the influence of mixing mechanism on internal flow dynamics.

Qian et al. [9] reported a numerical study of internal flow in a pressure swirl atomizer. The interface of liquid and air is modeled by VOF technique. The technique

called coupled level set/VOF solver is used for numerical modeling. The impact of different geometric parameters on atomization quality is reported. The numerical prediction of the internal flow field, spray cone angle, and velocity profiles are compared to the published literature. The comparison shows that the coupled level set/VOF method is able to predict the flow pattern more accurately than the conventional VOF method.

Cui et al. [10] visualized the internal flow in a pressure swirl atomizer and characterized the effect of orifice geometry on spray and flow field. Interferometer particle imaging (IPI) is used for droplet size measurement. The experiments are performed using water. The nozzles are manufactured from transparent methyl methacrylate. The effect of the flow field in different nozzles having manufacturing deviations under various injection pressures is reported. The Sauter mean diameter (SMD) of drops monotonously decreases with an increase in injection pressures.

The objectives of this study are to design a pressure swirl atomizer for use in an 1100-kW class aero-derivative gas turbine engine and to explore the possibility of additive manufacturing of atomizer by 3D printing. In case the 3D printing is not successful, it is planned to manufacture the atomizer by conventional machining methods and carry out numerical modeling of internal flow. The numerical results obtained are validated by experiments.

25.3 Governing Equations

The governing equations of fluid flow provide mathematical statements of the laws of conservation of physics. These are the continuity equation and momentum conservation equations. These equations are solved over the problem domain to obtain the instantaneous values of flow field variables [11].

These fluid flow governing equations are;

Continuity equation:

$$\frac{\partial \rho}{\partial t} + \nabla \cdot (\rho V) = 0 \tag{25.1}$$

X-momentum:

$$\frac{\partial (\rho u)}{\partial t} + \nabla \cdot (\rho u V) = -\frac{\partial p}{\partial x} + \frac{\partial \tau_{xx}}{\partial x} + \frac{\partial \tau_{yx}}{\partial y} + \frac{\partial \tau_{zx}}{\partial z} + \rho q_x \tag{25.2}$$

Y-momentum:

$$\frac{\partial (\rho v)}{\partial t} + \nabla \cdot (\rho v V) = -\frac{\partial p}{\partial y} + \frac{\partial \tau_{xy}}{\partial x} + \frac{\partial \tau_{yy}}{\partial y} + \frac{\partial \tau_{zy}}{\partial z} + \rho q_y \tag{25.3}$$

Z-momentum:

$$\frac{\partial(\rho w)}{\partial t} + \nabla \cdot (\rho w V) = -\frac{\partial p}{\partial z} + \frac{\partial \tau_{xz}}{\partial x} + \frac{\partial \tau_{yz}}{\partial y} + \frac{\partial \tau_{zz}}{\partial z} + \rho q_z \qquad (25.4)$$

Apart from solving the continuity and momentum conservation equations, the interphase of the fuel and air is tracked by the solution of continuity equation for volume fraction of the fuel.

$$\frac{1}{\rho_b}\left[\frac{\partial}{\partial t}(\beta_b \rho_b) + \nabla \cdot (\beta_b \rho_b \vec{\upsilon})\right] = \sum_{p=1}^{n} \dot{m}_{ab} - \dot{m}_{ba} \qquad (25.5)$$

The volume fraction (β) of each finite volume is specified as

$$\beta = \begin{cases} 1 & \text{pure liquid (fuel)} \\ 0 < \beta < 1, & \text{gas−liquid interface} \\ 0 & \text{pure gas (air)} \end{cases}$$

The volume fraction of the bth liquid phase is calculated based on the constraint,

$$\sum_{b=1}^{n} \beta_b = 1 \qquad (25.6)$$

25.4 Design of Atomizer

Radcliffe [12] did extensive research on the effect of geometrical parameters on atomization quality using a simplex atomizer. A large number of swirl atomizers with different geometric sizes are tested with water, and the results are published. These atomizers have two fixed parameters, the diameter of the swirl chamber (D) and swirl chamber cone angle (φ). The other geometric parameters are presented in Table 25.1.

The atomizer has a body, housing the swirl pin. The swirl pin is located centrally inside the body by a compression spring. A fuel filter normally of 10 μm mesh size is placed at the inlet of the atomizer and locked with a circlip. The swirl pin has three inclined swirl ports in such a way that the liquid enters the chamber with sufficient swirl velocity component. The schematic drawing of the atomizer is shown in Fig. 25.1. Figure 25.2 shows the sectional view of atomizer housing. Isometric view and front view of swirl pin are shown in Fig. 25.3.

**Table 25.1** Atomizer design parameters

Parameters	Values
Orifice diameter	$d = 0.6$ mm
Swirl chamber diameter	$D = 6d$
Size of tangential port	$P = 0.5 \times 0.5$ mm
Length of final orifice	$t = 2d/3$
Length of cylindrical section of swirl chamber	$b = 2d$
Radius of offset of tangential ports	$r = D/2 - 3d/4$
Swirl chamber cone angle	$\Phi = 90°$

Fig. 25.1 Schematics of swirl atomizer
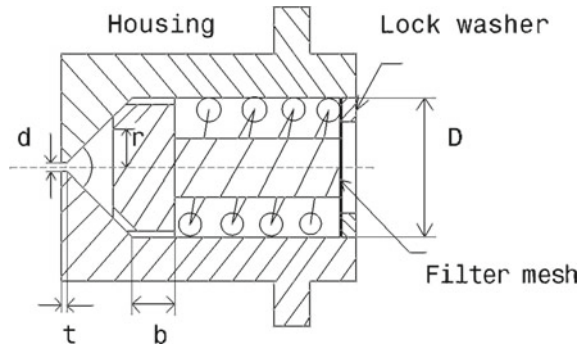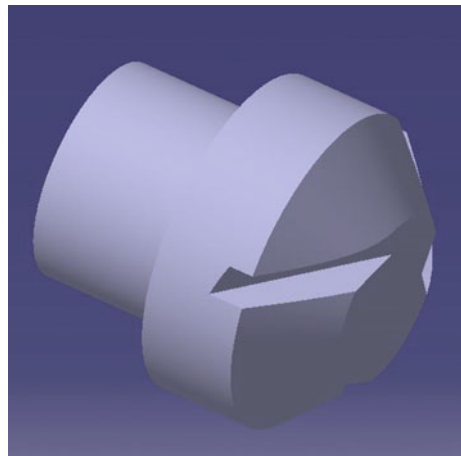

Fig. 25.2 Sectional view of atomizer housing
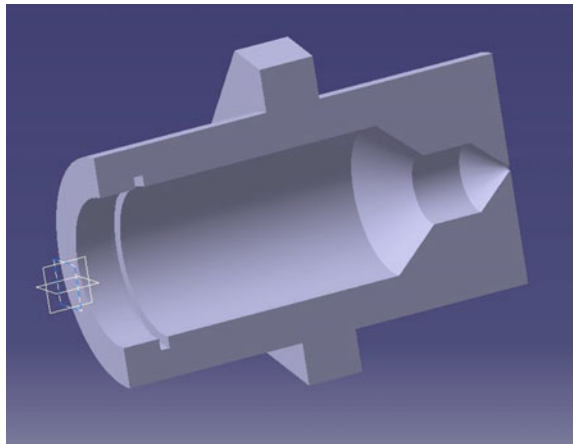
Fig. 25.3   Swirl pin
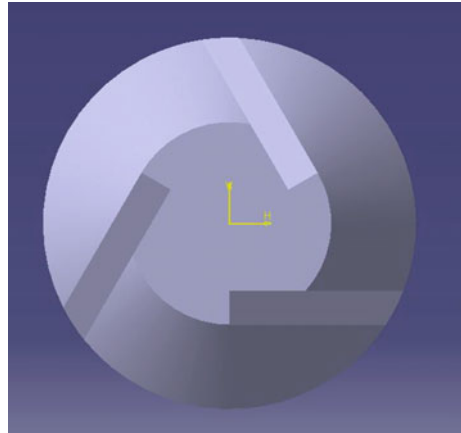
(a) Front view

(b) Isometric view

25.5   Rapid Prototyping and Manufacturing

25.5.1   Introduction

The term rapid prototyping and manufacturing (RP&M) is synonymously used for 3D printing. The earlier application of the technology was limited to manufacturing of prototypes. The earlier technology has not led to the manufacturing of functional parts. The 3D printing industry is fast maturing and opening up several avenues in manufacturing functional parts. The prototype provides an excellent visualization than a hundred pictures. The rapid prototyping makes the process of verification of design easier to examine whether the prototype carries all the desired features

and it carries any unwanted features. Though functional tests are not performed, the designers are able to hold in their hands the geometrically verified parts.

25.5.2 Methods of 3D Printing

The stereolithography (SLA) was developed by a Japanese researcher Dr. Hideo Kodama during early 1980. The process uses ultraviolet light to cure the photosensitive polymer in layer-by-layer additive manufacturing. Several distinct additive manufacturing processes have been evolved, and they differ in the method of layering, materials, and machines used. The early development of fused deposition modeling (FDM) has confined mostly to desktop platforms. This process has limitations since precision and repeatability are major concerns which prevent the applicability of the process in professional applications.

The selective laser sintering (SLS) or direct metal laser sintering (DMLS) is based on the selective fusion of a powder bed in layers as per the CAD model. The plastic-based process is referred to as SLS, and the metal based process is referred to as DMLS.

The printing time in conventional SLS/DMLS is very prohibitive. The development of mask-image projection-based stereolithography (MIP-SL) has drastically reduced the manufacturing time of homogenous objects.

25.5.3 Aeronautical Industry and 3D Printing

Aeronautical industry is an early adopter of 3D printing compared to other industries. Functional parts used in aerospace and defense applications are generally required to be manufactured with close dimensional tolerances. Moreover, development of a new component by conventional methods takes generally longer time due to the complex nature of geometrical features and subjection of many quality certification processes. The 3D printing offers an excellent tool for quick manufacturing of not only the prototype but also the functional components.

Though the 3D CAD model and drawings give a reasonable understanding of the components, a quick made physical model cannot be supplemented by drawings. This makes 3D printing an attractive platform to understand the intricacy of complicated components in the early stages of development. The manufacturing of an aircraft or an aero-engine requires hundreds of fixtures and jigs. When these are 3D printed, it saves roughly 60–90% of cost and development time compared to other conventional manufacturing processes [13].

Surrogates are the components which represent actual components but are used for educational and training purposes. These surrogates are normally used on the production floor. The 3D printing can be adopted for the manufacture of surrogates.

3D printing is successfully applied in the manufacturing of low-volume structures and metal brackets. These include mounts of oil and fuel accessories on an aero-engine or mounts of complex life-saving systems in an aircraft. Other functional parts suitable for 3D printing are combustion liners, air intake, and exhaust ducts. Surface finish is a critical requirement in the aeronautical industry. The surface finish of 3D printed components is not suitable for ready to use. The surface finish of additive manufactured components has been improved by the development of material jetting and binder jetting technologies. These can offer smooth, injection-molding-like finish with a little post-processing.

Major aerospace companies like Rolls-Royce, Turbomeca, and GE are foraying into manufacturing of aero-engine components by 3D printing to save time, money, and inventory. Rolls-Royce has a plan to fly the largest 3D printed part ever flown; however, it has not set any time frame. Rolls-Royce has printed the front bearing housing for the Trent XWB-97 engine from titanium with 1.5 m diameter [14]. GE has already manufactured titanium structures and bearing housing using electron beam melting technology (EBMT) [15]. The Indian aeronautical industry is yet to go a long way in adopting 3D printing of aero-engine components or aircraft structures. Recently, Hindustan Aeronautics Limited has forayed into manufacturing of centrifugal pump casing and nozzle guide vanes of developmental projects. However, these parts are yet to undergo a long certification process.

25.5.4 Raw Materials for 3D Printing

There are a variety of raw materials available for 3D printing. The selection of the right material for the intended application needs an extensive research. The acrylonitrile butadiene styrene (ABS) and polylactic acid (PLA) are most commonly used materials for preliminary research works. ABS belongs to thermoplastic polymer family and opaque. ABS is more popular because of its superior plastic properties. The major advantages of ABS are its abrasion resistance and affordability. The added advantages are its impact strength and lightweight. The melting temperature is 200 °C which makes ABS an ideal choice for use in safe machines. It is fire-retardant and also gives good surface quality. It is biocompatible and recyclable. However, oxidation of ABS at higher temperatures leads to yellowing color.

PLA is considered as an alternative to ABS. It is made from cornstarch. It melts at 150 °C. The PLA prints made for mechanical operations or when stored at high temperatures result in warping, cracking, or melting. It is also biodegradable.

Metal printing is the fastest growing segment in the rapid prototyping industry. The availability of low-cost metal powders is directly tied to the realization of potential and transformation of industrial production. Metal powders are generally manufactured either by water jet atomization or gas atomization. Gas-atomized powders are generally preferred over the water-jet-atomized powders because the later one produces irregularly shaped powders.

25.5.5 3D Printing of Atomizer

The swirl pin and the housing are the two important components of a pressure swirl atomizer. The accuracy and surface quality of fuel inlet ports on the swirl pin are the most important for achieving proper atomization. It is decided to manufacture these two components by 3D printing using FDM with ABS material. The print parameters are listed in Table 25.2.

The print quality of atomizer housing is better than the quality of swirl pin. The 3D printing has failed to print the 0.5×0.5 mm fuel inlet port at the swirl pin. The surface finish has not improved even after post-print cleaning, making the 3D printed components unsuitable for functional testing. The model is built in 0.12-mm-thick layers which is the minimum possible thickness by FDM. The finest feature of the swirl pin, the fuel inlet port 0.5×0.5 mm size is not printed by the chosen printing method. After a careful market research, 0.178-mm-diameter nozzle is used for printing. The chosen nozzle is the smallest size found in the market at present. The 3D printed swirl pin is shown in Fig. 25.4.

Subsequently, the atomizer housing and swirl pin are manufactured by wire cut electric discharge machining. Figure 25.5 shows the swirl pin manufactured by sub-

Table 25.2 Parameters of 3D printing

Model material	ABS
Model volume	50.0 mm^3
Filament diameter and length	1.00 and 30.00 mm
Diameter of print nozzle	0.2 mm
Temperature of nozzle tip	315 °C
Printer oven temperature	90 °C

**Fig. 25.4** Swirl pin, 3D printed

Fig. 25.5 Swirl pin

tractive manufacturing. The stainless steel of grade SS347 is used for both housing and swirl pin. The swirl pin is assembled inside the housing using a compression spring, filter, and a circlip.

25.6   Numerical Modeling of Atomization

The 3D fluid flow domain is shown in Fig. 25.6. However, the atomizer internal flow analysis is performed in 2D axisymmetric model. The 2D model is discretized with mapped face mesh, Fig. 25.7. The computational domain is extended up to 2.00 mm down the orifice to study the spray structure.

The atomizer internal flow is classified as stratified where the two immiscible fluids, fuel and air are separated by a clearly defined interface boundary. The fluid mechanics offers two different approaches of mathematical modeling of multiphase flow, viz. Euler–Lagrange approach and Euler–Euler approach. The Euler–Euler approach assumes the phases are interpenetrating continua in this case fuel and air. This approach introduces a concept called phasic volume fraction since the volume of a phase is unique and cannot be occupied by any other phase. The VOF model is an interface surface tracking technique based on the Euler–Euler approach. There are certain limitations in using the VOF model. The model can only be used with pressure-based solver, and the control volume is always occupied by either of a phase in the case of two-phase flow. The thermophysical properties of Jet A used in the analysis are presented in Table 25.3.

The convection terms of the governing equations are discretized with least square cell-based method. The pressure equation is discretized with pressure staggering option (PRESTO) scheme. The momentum and swirl velocity equations are discretized with the second-order upwind scheme. The volume fraction equation is discretized with the first-order upwind scheme. The first-order implicit scheme is
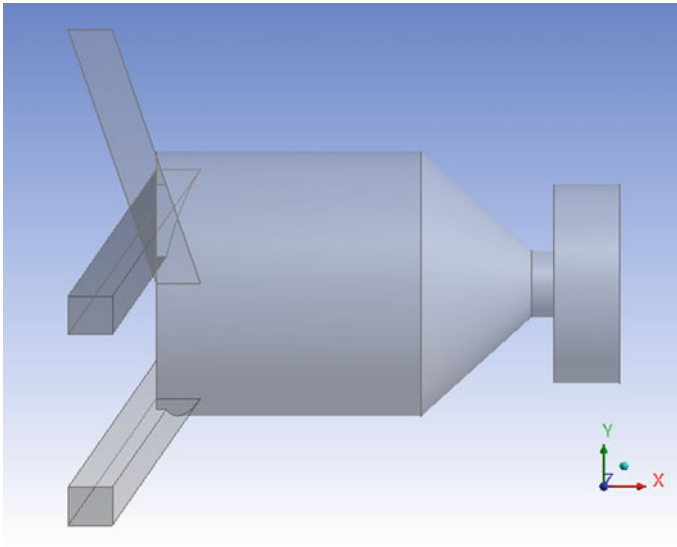
Fig. 25.6 Fluid flow model, 3D
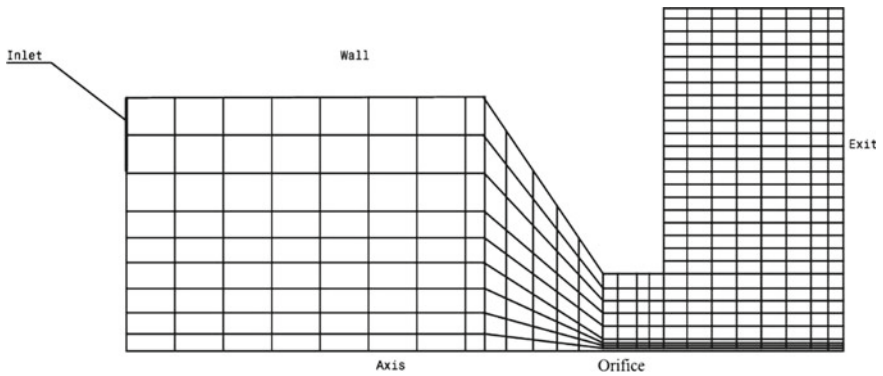
Fig. 25.7 Representative 2D axisymmetric model

Table 25.3 Thermophysical properties of Jet A	
Fuel flow rate	0.0069 kg/s
Fuel inlet direction vector	$0.18\,j - 0.98\,k$
Density	800 kg/m^3
Upstream pressure	3.0, 4.0, 5.0 MPa
Downstream pressure	100 kPa
Surface tension	0.026 N/m
Dynamic viscosity	0.0067 kg/m-s
Fuel temperature	300 K

Table 25.4 Details of mesh independency study

Case	Minimum edge size (μm)	Mesh count (M)	Spray cone (°)
Case 1	2.0	0.065	60
Case 2	1.6	0.100	60
Case 3	1.5	0.125	60

applied for discretizing transient formulation. All the flow field variables and volume fraction in the problem domain are transiently solved using pressure-based and coupled solver scheme. The time step of 1.0 μs is maintained throughout the transient solution procedure. The solution process is repeated for three upstream pressures 3.0, 4.0, and 5.0 MPa. The mesh independence study is performed on consecutively refined meshes. The details are presented in Table 25.4.

There are no appreciable improvements when the control volume is refined with finer meshes. Hence, the results obtained from Case 1 alone are considered for further discussion.

25.7 Testing of Atomizer

The atomizer after assembly is tested in a laboratory-scale atmospheric test facility using aviation jet fuel. The test setup has a fuel tank mounted on wheels with a pump fixed over it. The tank mounted fuel pump circulates the fuel to the test chamber. A pressure regulator is provided to adjust the supply pressure, according to the test requirements. A flow controller controls the flow rate. The drain line takes the fuel from the test chamber to the fuel storage tank through a suitable filtering mechanism. The fuel is collected in a measuring jar, and the flow rate is maintained as per the test requirements. A temperature indicator indicates the temperature of inlet fuel. The measuring jars are used to maintain the design fuel flow rate. The schematic diagram of the stand-alone atomizer test facility and the test stand are shown in Figs. 25.8 and 25.9. Table 25.5 shows the test parameters.

The fuel supply system is a centralized facility which can be used for many other requirements. The atomizer test facility is as a stand-alone unit. The test chamber can be separated from the fuel supply system. The atomizer is fitted in the downward direction. The facility can be used to test a single atomizer or a set of 16 atomizers simultaneously, and the fuel supply can be adjusted according to the requirement.

25.8 Results and Discussion

The prediction of flow field variables and spray cone structures under 3.0, 4.0, and 5.0 MPa injection pressures are studied. There are no appreciable differences in the results. Though the results show regular increasing trends in velocity fields for
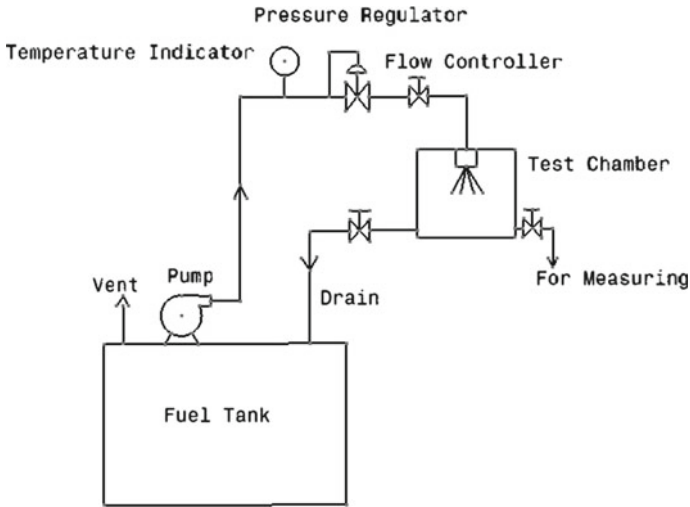
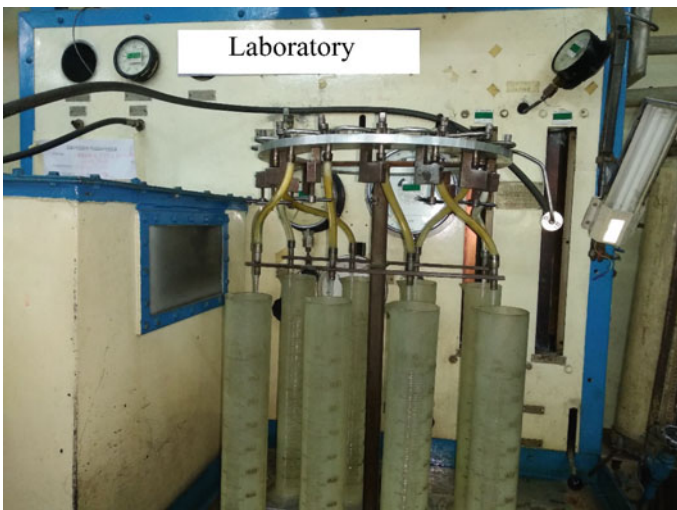**Fig. 25.8** Schematic diagram of a stand-alone atomizer test facility

Fig. 25.9 Atomizer test stand

increasing injection pressures, the spray patterns remain nearly the same for all injection pressures. Three locations are chosen to study the velocity profiles, viz. 1.0 and 2.0 mm from the fuel inlet, and both fall inside the swirl chamber. The third location 4.0 mm from the fuel inlet falls just outside the orifice. Figures 25.10, 25.11, and 25.12 show the instantaneous axial, radial, and swirl velocity profiles along the swirl chamber and at the near exit of the orifice. There is no much variation in axial and radial velocity inside the swirl chamber. At the near exit of the orifice, there

Table 25.5 Atomizer test parameters

Fuel	Jet A
Flow rate	0.0069 kg/s
Upstream pressure	3.0, 4.0, 5.0 MPa

is a strong gradient in swirl velocity observed. The axial distance has no impact on swirl velocity inside the swirl chamber [16]. The swirl velocity at the orifice exit is zero approximately at 2/3rd height from the atomizer axis. This confirms the disintegration of the liquid sheet just after leaving the orifice.

The stream function plot, Fig. 25.13, confirms there is no mass flow in the air core region and inside the hollow cone spray. The plot also indicates that the region just at the beginning of nozzle converging zone experiences zero mass flow. The wrinkles at the beginning of the air core are clearly captured as reported by Sumer et al. [17]. The stream function plot also confirms that the flow inside the swirl chamber is highly stratified. The formation of Rankine vortex is confirmed from streamlines plot shown in Fig. 25.14.

The contour plot showing volume fraction of fuel confirms the formation of hollow cone spray measuring approximately 60°. as per the design, Fig. 25.15. The air core does not exhibit uniform size and is unstable in the beginning. It is minimum at the beginning and gradually increases to 0.4 mm at the end of the orifice. The spray sheet thickness is approximately measuring 0.10 mm.
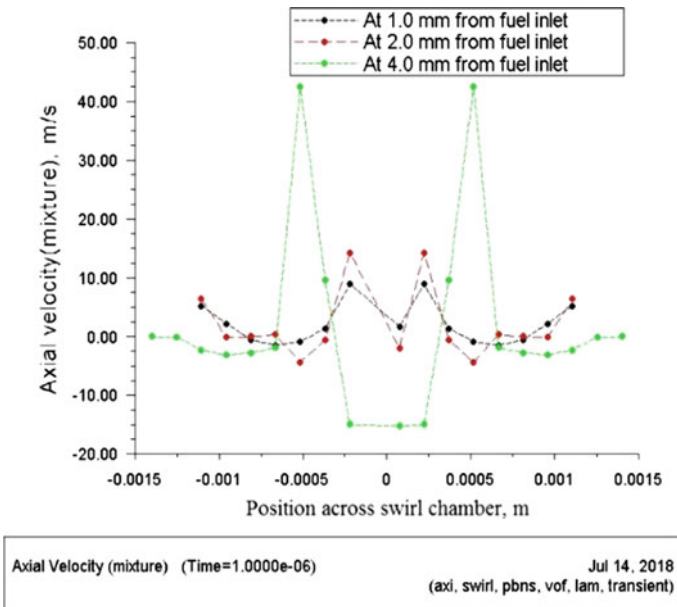
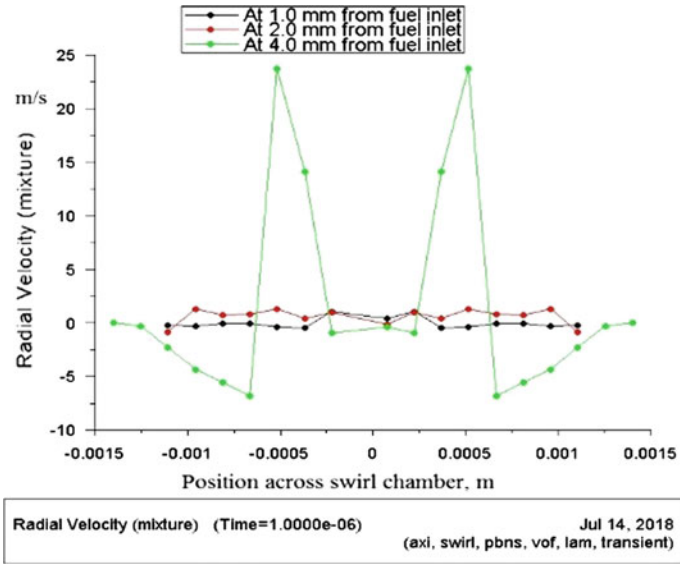**Fig. 25.10** Axial velocity, 3.0 MPa upstream pressure

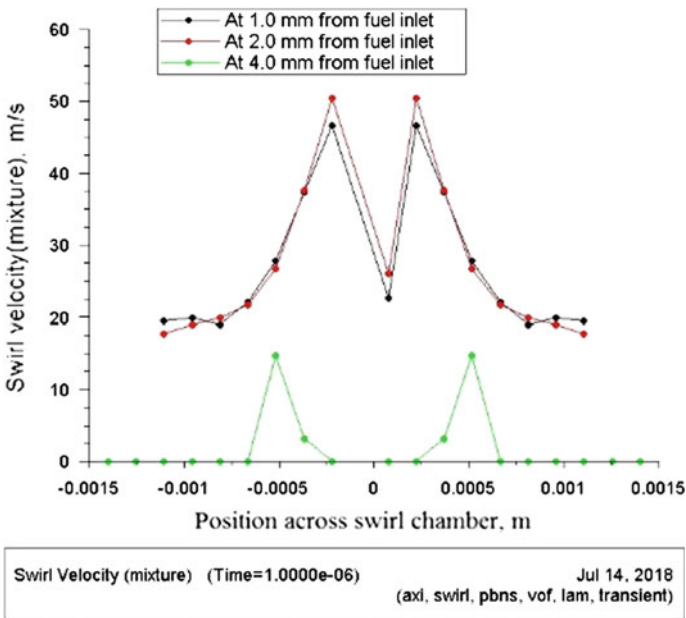**Fig. 25.11** Radial velocity, 4.0 MPa upstream pressure

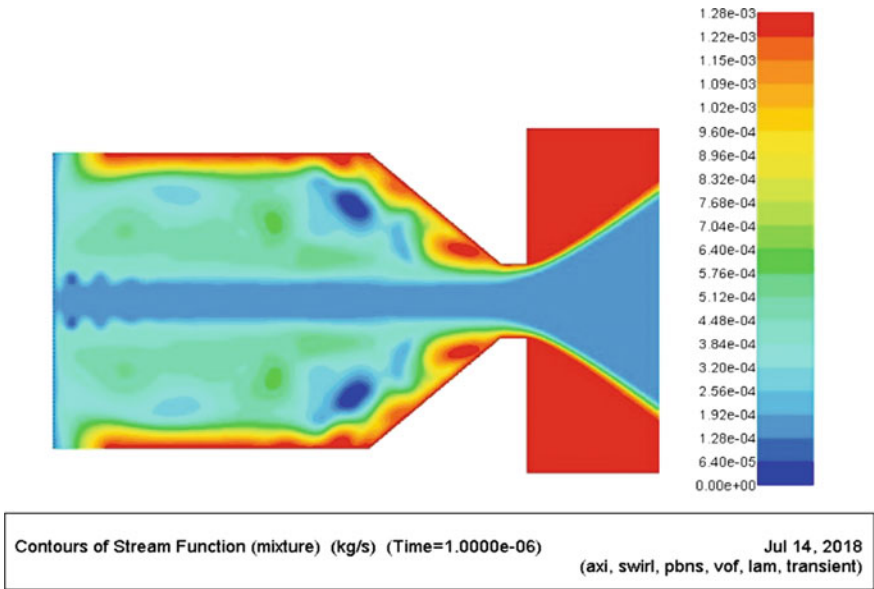**Fig. 25.12** Swirl velocity, 5.0 MPa upstream pressure
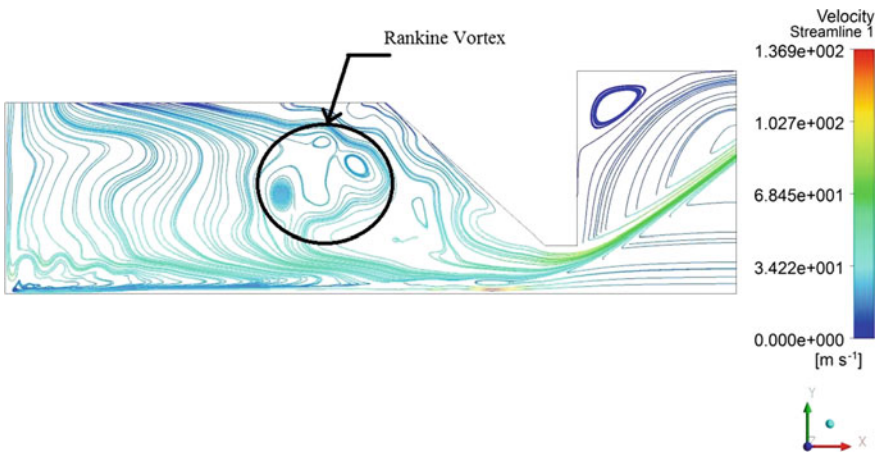
Fig. 25.13   Stream function showing air core at the center
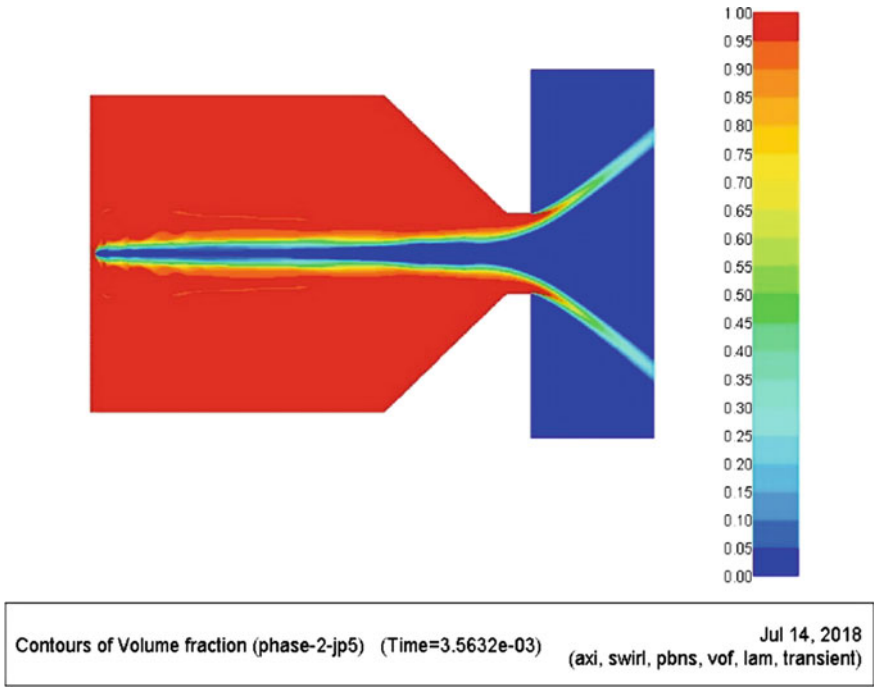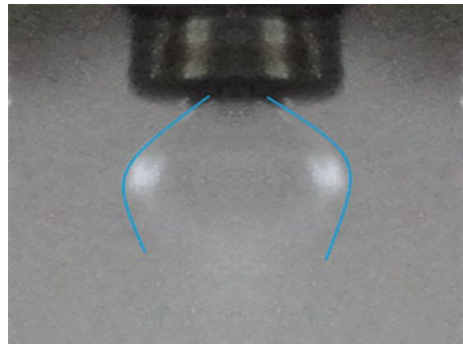

Fig. 25.14   Streamlines

Fig. 25.15 Hollow cone spray

**Fig. 25.16** Hollow cone spray at low pressure

During testing of atomizer performance, at a low injection pressure, onion-shaped spray is observed. With the gradual increase in pressure, the onion-shaped spray transforms into a full-fledged stable hollow cone spray, Figs. 25.16 and 25.17. The spray cone angle is measured by capturing the image of the spray by a high-speed digital single-lens reflex camera (DSLR) with a 50.00-mm f1.8 lens. The spray structures observed during experimentation are similar to those reported by Moon et al. [18].

Fig. 25.17 Stable
atomization at high pressure

Fig. 25.18 Jet penetration
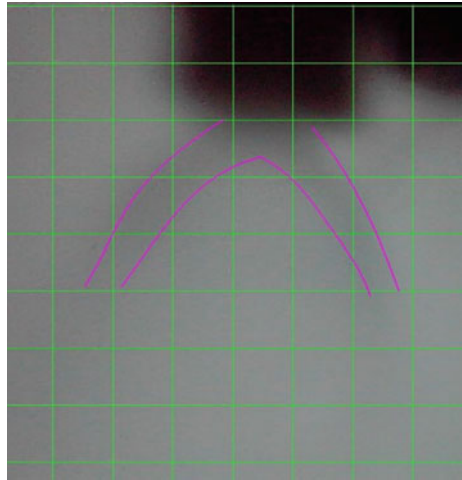
The jet penetration is not clearly visible due to the presence of fuel mist inside the test chamber. The jet sheet is visible approximately about 3.0–4.0 mm as measured from a shadowgraph, Fig. 25.18. The jet breakup is almost similar to the one reported by Garai et al. [19].

25.9   Conclusion

The pressure swirl atomizer is designed for the intended application. An attempt is made to manufacture the atomizer by 3D printing using fused deposition modeling. The method failed to print the smallest geometrical feature like tangential fuel inlet port of swirl pin. The atomizer housing is also manufactured by 3D printing. However, the surface quality is not good enough, even after sufficient post-print cleaning. The 3D printed swirl pin and housing are not taken up for further functional testing.

Hence, the atomizer is manufactured by wire cut electrical discharge machining. The atomizer internal flow is modeled by solving unsteady Navier–Stokes equations over the 2D axisymmetric model. The air–fuel interface is tracked by solving the continuity equation for fuel volume fraction using the volume of fluid model of a commercial computational fluid dynamics code. The model is able to predict the flow field variables with reasonable accuracy. Also, the model is able to capture the air core formation and hollow cone spray structures. The atomizer is tested with Jet A fuel. The spray cone structure is compared to numerical prediction and to the published literature. The numerically predicted velocity fields are compared to previously published research work. No appreciable contradiction is noticed. The direct metal laser sintering is fast catching-up as the most preferred 3D printing choice in aerospace applications because of its ability to build the part by layer as thin as 20 μm using metal powders. This makes the process more suitable not only for manufacturing prototypes, but also functional parts. However, certain limitations like thermal distortion, porosity, surface roughness, and cost of DMLS printed parts need to be addressed thoroughly.

References

1. Lefebvre, A.H., Ballal, D.R.: Gas Turbine Combustion Alternative Fuels and Emissions. CRC Press, Boca Raton, FL (2013)
2. Winterfeld, G., Eickhoff, H.E., Depooter, K.: Combustion system design. In: Mellor, A.M. (ed.) Design of Modern Turbine Combustor. Academic Press, London (1990)
3. Hansen, K.G., Madsen, J., Trinh, C.M., Ibsen, C.H., Solberg, T., Hjertager, B.H.: A computational and experimental study of the internal flow in a scaled pressure-swirl atomizer. In: ILASS-Europe 2002 (2002)
4. Rezaeimoghaddam, M., Elahi, R., Razavi, M.R.M., Ayani, M.B.: Modeling of non-newtonian fluid flow within simplex atomizers. In: Proceedings of the ASME 2010 10th Biennial Conference on Engineering Systems Design and Analysis ESDA2010, Turkey, 2010
5. Ma, Z.: Investigation on the internal flow characteristics of pressure-swirl atomizer. Ph.D. Thesis, University of Cincinnati, Department of Aerospace Engineering and Engineering Mechanics of the College of Engineering (2001)
6. Marchione, T., Allouis, C., Amoresano, A., Beretta, F.: Experimental investigation of a pressure swirl atomizer spray. J. Propuls. Power **23**(5) (2007)
7. Fu, Q.: Numerical simulation of the internal flow of swirl atomizer under ambient pressure. J. Mech. Eng. Sci. **0**(0) (2015)
8. Mkvik, M., Smolar, M., Olsiak, R.: Numerical investigation of the twin-fluid atomizers internal flows. In: AIP Conference Proceedings 1768, 2016
9. Qian, W., Hui, X., Zhang, C., Xu, Q., Lin, Y.: A numerical study of the internal flow in a pressure swirl atomizer. In: Proceedings of ASME Turbo Expo 2017: Turbomachinery Technical Conference and Exposition GT2017, USA, 2017
10. Cui, J., Lai, H., Li, J., Ma, Y.: Visualization of internal flow and the effect of orifice geometry on the characteristics of spray and flow field in pressure-swirl atomizers. Appl. Therm. Eng. http://dx.doi.org/10.1016/j.applthermaleng.2017.08.103

11. Versteeg, H.K., Malalasekera, W.: An Introduction to Computational Fluid Dynamics the Finite Volume Method, Pearson, India (2007)
12. Radcliffe, A.: The performance of a type of swirl atomizer. Proc. Inst. Mech. Eng. **69**(1) (1995)
13. https://www.3dhubs.com/knowledge-base/aerospace-3d-printing-applications. Accessed 28 Aug 2018
14. https://www.theengineer.co.uk/issues/june-2015-digi-issue/rolls-royce-breaks-additive-record-with-printed-trent-xwb-bearing. Accessed 17 June 2018
15. http://www.arcam.com/technology/electron-beam-melting. Accessed 16 June 2018
16. Maly, M., Sapik, M., Jedelsky, J., Janackova, L., Jicha, M., Slama, J., Wigley, G.: Internal flow characteristics in scaled pressure-swirl atomizer. In: EPJ Web of Conference 180, 2018
17. Sumer, B., Erkan, N., Uzol, O., Tuncer, I.H.: Experimental and numerical investigation of a pressure swirl atomizer. In: 12th Triennial International Conference on Liquid Atomization and Spray Systems, Germany, 2012
18. Moon, S., Abo-Serie, E., Bae, C.: Air flow and pressure inside a pressure-swirl spray and their effects on spray development, Exp. Therm. Fluid Sci. **33**(2) (2009)
19. Garai, A., Pal, S., Mondal, S., Ghosh, S., Sen, S., Mukhopadhyay.: A Experimental investigation of spray characteristics of kerosene and ethanol-blended kerosene using a gas turbine hybrid atomizer. Sadhana **42**(4) (2017)